

Study on Standard Mathematical Model of Pure Loss of Stability in Stern-quartering Waves

Jiang Lu, *China Ship Scientific Research Center, Wuxi, China, lujiang1980@aliyun.com*

Min Gu, *China Ship Scientific Research Center, Wuxi, China, gumin702@163.com*

ABSTRACT

The guidelines for direct stability assessment of pure loss of stability are currently under development at the International Maritime Organization (IMO) for the second generation intact stability criteria. The present study intends to provide a standard mathematical model for predicting pure loss of stability, with sufficient accuracy and practically useful. Firstly, one Maneuvering Modeling Group (MMG) standard method for ship maneuvering predictions is referenced with the roll motion and heel-induced hydrodynamic forces taken into account. Secondly, existing mathematical models for broaching predictions are introduced into the standard mathematical model for predicting pure loss of stability. Finally, some crucial terms for predicting pure loss of stability in stern-quartering waves are numerically investigated with the ONR tumblehome vessel which is one of standard ship models for the second generation intact stability criteria, and some remarks are given for the standard mathematical model of pure loss of stability in stern-quartering waves.

Keywords: *Pure loss of stability, second generation intact stability criteria, MMG, broaching, ONR tumblehome.*

LIST OF SYMBOLS

a_H Rudder force increase factor
 AE, FE After section and forward section
 A_R Rudder area
 $A_{R\sigma}, A_{R\delta}$ The port and starboard rudder area
 $B(x)$ Sectional breadth
 C_T Total resistance coefficient in calm water
 d Ship draft
 $d(x)$ Sectional draught
 D_p Propeller diameter
 $D(p)$ Roll damping moment
 F_N Rudder normal force
 F_n Froude number based on ship length
 f_α Rudder lifting slope coefficient
 g Gravitational acceleration
 GM Metacentric height
 GZ_W Righting arm in waves
 H_R Rudder span length
 I_{xx}, J_{xx} Moment and add moment of inertia in roll
 I_{zz}, J_{zz} Moment and add moment of inertia in yaw
 J_p Propeller advanced ratio
 k Wave number

K_r, N_r, Y_r Derivative of roll moment, yaw moment and sway force with respect to yaw rate, their nondimensional K'_r, N'_r, Y'_r
 K_{rr}, N_{rr}, Y_{rr} Derivative of roll moment, yaw moment and sway force with respect to cubic yaw rate, their nondimensional $K'_{rr}, N'_{rr}, Y'_{rr}$
 $K_{r|\dot{\varphi}}, N_{r|\dot{\varphi}}, Y_{r|\dot{\varphi}}$ Derivative of roll moment, yaw moment and sway force with respect to yaw rate and heeling angle, their nondimensional $K'_{r|\dot{\varphi}}, N'_{r|\dot{\varphi}}, Y'_{r|\dot{\varphi}}$
 K_{rr}, N_{rr}, Y_{rr} Derivative of roll moment, yaw moment and sway force with respect to squared yaw rate and sway velocity, their nondimensional $K'_{rr}, N'_{rr}, Y'_{rr}$
 K_{rr}, N_{rr}, Y_{rr} Derivative of roll moment, yaw moment and sway force with respect to squared yaw rate and sway velocity, their nondimensional $K'_{rr}, N'_{rr}, Y'_{rr}$
 K_v, N_v, Y_v Derivative of roll moment, yaw moment and sway force with respect to sway velocity, their nondimensional K'_v, N'_v, Y'_v
 K_{vv}, N_{vv}, Y_{vv} Derivative of roll moment, yaw moment and sway force with respect to cubic sway velocity, their nondimensional $K'_{vv}, N'_{vv}, Y'_{vv}$

$K_{\dot{v} \phi}, N_{\dot{v} \phi}, Y_{\dot{v} \phi}$	Derivative of roll moment, yaw moment and sway force with respect to sway velocity and heeling angle, their nondimensional $K'_{\dot{v} \phi}, N'_{\dot{v} \phi}, Y'_{\dot{v} \phi}$	X_R, Y_R, N_R, K_R	Surge force, lateral force, yaw moment and roll moment around center of ship gravity by steering
K_ϕ, N_ϕ, Y_ϕ	Derivative of roll moment, yaw moment and sway force with respect to roll angle, their nondimensional $K'_\phi, N'_\phi, Y'_\phi$	X_{rr}	Derivative of surge force with respect to squared yaw rate, its nondimensional X'_{rr}
K_p	Rudder gain	X_{vr}	Derivative of surge force with respect to sway velocity and yaw rate, its nondimensional X'_{vr}
K_T	Thrust coefficient of propeller	X_{vv}	Derivative of surge force with respect to squared sway velocity, its nondimensional X'_{vv}
L_{pp}	Ship length between perpendiculars	X_{vvvv}	Derivative of surge force with respect to 4th order sway velocity, its nondimensional X'_{vvvv}
ℓ_R'	Correction factor for flow-straightening due to yaw	X_w, Y_w, N_w, K_w	Surge force, lateral force, yaw moment and roll moment around center of ship gravity acting on ship hull induced by waves
m	Ship mass	Z_H	Vertical position of center of sway force due to lateral motion
m_x, m_y	Added mass in surge and sway	Z_{HR}	Vertical position of additional lateral force due to rudder
n_p	Propeller revolution number	Z_R	Vertical position of center of rudder
OG	Vertical distance between center of gravity and waterline	α	Linear roll damping coefficient
P	Roll rate	α_R	Effective inflow angle to rudder
r	Yaw rate	β	Hull drift angle
R	Ship resistance	δ	Rudder angle
$S(x)$	Sectional area	η	Ratio of propeller diameter to rudder span
$S_y(x)$	Added mass of one section at sway direction	ε	Ratio of wake fraction at propeller and rudder position
$S_{y\eta}(x)$	Added moment of one section at roll direction	κ	Propeller-induced flow velocity factor
S_F	Wetted hull surface area	λ	Wave length
t_p	Thrust deduction factor	Λ	Rudder aspect ratio
t_R	Steering resistance deduction factor	φ	Roll angle
T	Propeller thrust	γ	Cubic nonlinear roll damping coefficient
T_E	Time constant for steering gear	γ_R	Flow-straightening effect coefficient
T_D	Time constant for differential control	θ	Pitch angle
T_ϕ	Natural roll period	χ	Yaw angle from wave direction
u, v	Surge and sway velocity	χ_c	Yaw angle of auto pilot course
u_R	Longitudinal inflow velocity component to rudder	ρ	Water density
U	Ship forward velocity	ω	Wave frequency
w_p	Wake fraction at propeller position	ω_e	Averaged encounter frequency
w_R	Wake fraction at rudder position	ξ_G	Longitudinal position of center of ship gravity from a wave trough
W	Ship weight	(ξ_G, η_G, ζ_G)	Position of center of ship gravity in the space-fixed coordinate system
x_{HR}	Longitudinal position of additional lateral force due to rudder	ζ_w	Wave amplitude
x_R	Longitudinal position of rudder		
X_H, Y_H, N_H, K_H	Surge force, lateral force, yaw moment and roll moment around center of ship gravity acting on ship hull		
X_p	Surge force due to propeller		

1. INTRODUCTION

The guidelines for direct stability assessment of five stability failure models including pure loss of stability are under development at the International Maritime Organization (IMO) for the second generation intact stability criteria (IMO SDC 4, 2017). Once the crest of the large wave passes the midship section of a ship with a slightly higher speed than ship speed, the state of stability loss at the crest may exist long enough to evolve a large heel angle, or even capsizing. It is urgently required to establish a standard mathematical model which is sufficient accuracy and practically useful for predicting pure loss of stability in stern-quartering waves.

Without external heel moment, once the wave crest passes the ship, the ship will finally return to the upright position with regained stability except for cases that the ship already heel too far or the metacentric height in the wave is negative. Roll moment excited by oblique waves and heel moments induced by a centrifugal force due to ship maneuvering motions are the relevant external moments. Several freely running experiments also prove that coupling with maneuvering motion is essential for explaining the forward speed effect on pure loss of stability in stern-quartering waves (IMO SDC 3, 2016).

Pure loss of stability in stern-quartering waves is a nonlinear phenomenon involving large amplitude roll motion and it is still difficult to be predicted quantitatively. Japan delegation (IMO SLF55, 2013) notes that predicting pure loss of stability with their newly 4 degrees of freedom (DOF) mathematical model is more accuracy than the 2 DOF mathematical model (Kubo et al., 2012). The delegations for the second generation intact stability criteria at IMO SDC4 gave top priority to discussing the guidelines for direct stability assessment and the 4 DOF for predicting pure loss of stability has been agreed at the current stage (IMO SDC 4, 2017).

Though the 4 DOF mathematical model for predicting pure loss of stability has not been investigated widely with simulations and experiments, a 4 DOF mathematical model for broaching prediction (Umeda, 1999) has been investigated for many years. For providing a accurate mathematical model for broaching

prediction, Umeda and Hashimoto had investigated essential terms in the 4 DOF mathematical model one by one by utilizing fishing vessels. Nonlinear maneuvering forces in calm water (Umeda & Hashimoto, 2002), wave effect on linear maneuvering forces, roll restoring and rudder force (Umeda et al., 2003), and several nonlinear factors were also investigated, such as nonlinear wave forces, nonlinear sway-yaw coupling, wave effect on propeller thrust, heel-induced hydrodynamic forces for large heel angle in calm water (Hashimoto et al., 2004), and wave effect on heel-induced hydrodynamic forces for large heel angle. A simplified mathematical model was proposed for more practically useful (Hashimoto et al., 2011a). Existing 4 DOF mathematical model was used for broaching prediction of the ONR tumblehome vessel, and a fair quantitative prediction was realized (Hashimoto et al., 2011b). Broaching is a nonlinear phenomena related to ship maneuvering in the wave, and above 4 DOF mathematical models are based on a Maneuvering Modeling Group (MMG) model, but simulation methods without standard expressions could not be used in general. Therefore a MMG standard method for ship maneuvering predictions was introduced (Yasukawa & Yoshimura, 2015). A 4 DOF mathematical model was refined for broaching prediction of the ONR flare topside vessel (Umeda et al., 2016).

For drafting guidelines for direct stability assessment, several crucial elements for predicting parametric roll were investigated with simulations and experiments by the authors (Lu et al., 2017), and some crucial terms in the 4 DOF mathematical for predicting pure loss of stability still require further experimental and numerical studies with more examples, though the above 4 DOF mathematical models for broaching prediction have a certain degree of reference. The physical mechanism of pure loss of stability is different from that of broaching and a 4 DOF standard mathematical model for predicting pure loss of stability has not been established widely. Therefore, systematic studies on the 4 DOF mathematical model for predicting pure loss of stability are hot tasks at this stage. Also IMO is calling for the validation of numerical methods or guidelines for the finalization of second generation intact stability with examples.

Based on the MMG standard method and existing mathematical model for broaching and pure loss of stability, the present study intends to provide a 4 DOF standard mathematical model with unified expressions for the prediction of pure loss of stability. Some crucial terms in the mathematical model were investigated using one standard ship. The experiment is also in progress as the next step.

2. MATHEMATICAL MODEL

2.1 Coordinate systems

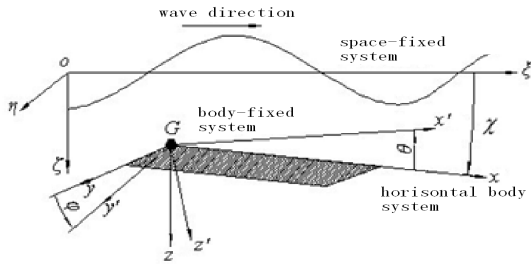


Figure 1: Coordinate systems

A space-fixed coordinate system $O-\xi\eta\zeta$ with the origin at a wave trough, a body-fixed system $G-x'y'z'$ with the origin at the center of gravity of the ship, and a horizontal body coordinate system (Hamamoto & Kim, 1993) $G-xyz$ which has the same origin with the body-fixed system but does not rotated around the x-axis and y-axis are adopted as shown in Fig.1.

The relationships between the horizontal body coordinate system $G-xyz$, the body-fixed system $G-x'y'z'$ and the space-fixed system $O-\xi\eta\zeta$ are shown in Eq. (1) and Eq. (2), respectively.

$$\begin{bmatrix} x \\ y \\ z \end{bmatrix} = \begin{bmatrix} \cos\theta & \sin\theta\sin\phi & \cos\phi\sin\theta \\ 0 & \cos\phi & -\sin\phi \\ -\sin\theta & \sin\theta\cos\phi & \cos\theta\cos\phi \end{bmatrix} \begin{bmatrix} x' \\ y' \\ z' \end{bmatrix} \quad (1)$$

$$\begin{bmatrix} \xi-\xi_G \\ \eta-\eta_G \\ \zeta-\zeta_G \end{bmatrix} = \begin{bmatrix} \cos\theta\cos\chi & \sin\phi\sin\theta\cos\chi & \cos\phi\sin\theta\cos\chi \\ & -\cos\phi\sin\chi & +\sin\phi\sin\chi \\ \cos\theta\sin\chi & \sin\phi\sin\theta\sin\chi & \cos\phi\sin\theta\sin\chi \\ & +\cos\phi\cos\chi & -\sin\phi\cos\chi \\ -\sin\theta & \sin\theta\cos\theta & \cos\theta\cos\theta \end{bmatrix} \begin{bmatrix} x' \\ y' \\ z' \end{bmatrix} \quad (2)$$

2.2 Mathematical model

Heave and pitch response will be dynamic or static depending on the encounter frequency. In case of astern waves, the encounter frequency is much lower than the natural frequencies of heave and

pitch so that coupling with heave and pitch is almost static (Matsuda & Umeda, 1997). The 4 DOF mathematical model are expressed by surge, sway, yaw and roll motions as shown in Eq. (3) to Eq. (6), respectively. Control equation for keeping course by steering is added in the 4 DOF mathematical model as shown in Eq. (7).

$$(m+m_x)\dot{u}-(m+m_y)vr = X_H + X_R + X_P + X_W \quad (3)$$

$$(m+m_y)\dot{v}+(m+m_x)ur = Y_H + Y_R + Y_W \quad (4)$$

$$(I_{zz} + J_{zz})\dot{r} = N_H + N_R + N_W \quad (5)$$

$$(I_{xx} + J_{xx})\dot{p} - m_x z_H ur - m_y z_H \dot{v} = K_H + K_R + K_W \quad (6)$$

$$-D(\phi) - WGZ_w(\xi_G / \lambda, \chi, \phi)$$

$$\dot{\delta} = \{-\delta - K_P(\chi - \chi_C) - K_P T_D r\} / T_E \quad (7)$$

The subscripts H, R, P and W refer to hull, rudder, propeller and wave, respectively.

2.3 Hydrodynamic forces acting on ship hull

Hydrodynamic forces acting on a ship hull of a MMG standard method (Yasukawa & Yoshimura, 2015) is referenced with the roll motion and heel-induced hydrodynamic forces taken into account.

The hull forces in still water X_H, Y_H, N_H and K_H are expressed as follows:

$$X_H = -R(u) + \frac{1}{2} \rho L_{pp} dU^2 (X'_{vv} \cdot v'^2 + X'_{vr} \cdot v'r' + X'_{rr} \cdot r'^2 + X'_{vvv} \cdot v'^3 + X'_{vvr} \cdot v'^2 r' + X'_{vrr} \cdot v'r'^2 + X'_{rrr} \cdot r'^3) \quad (8)$$

$$Y_H = \frac{1}{2} \rho L_{pp} dU^2 (Y'_v \cdot v' + Y'_r \cdot r' + Y'_{vv} \cdot v'^3 + Y'_{vr} \cdot v'^2 r' + Y'_{rr} \cdot v'r'^2 + Y'_{rrr} \cdot r'^3 + Y'_\phi \cdot \phi + Y'_{v|\phi} \cdot v'|\phi| + Y'_{r|\phi} \cdot r'|\phi|) \quad (9)$$

$$N_H = \frac{1}{2} \rho L_{pp}^2 dU^2 (N'_v \cdot v' + N'_r \cdot r' + N'_{vv} \cdot v'^3 + N'_{vr} \cdot v'^2 r' + N'_{rr} \cdot v'r'^2 + N'_{rrr} \cdot r'^3 + N'_\phi \cdot \phi + N'_{v|\phi} \cdot v'|\phi| + N'_{r|\phi} \cdot r'|\phi|) \quad (10)$$

$$K_H = \frac{1}{2} \rho L_{pp} d^2 U^2 (K'_v \cdot v' + K'_r \cdot r' + K'_{vv} \cdot v'^3 + K'_{vr} \cdot v'^2 r' + K'_{rr} \cdot v'r'^2 + K'_{rrr} \cdot r'^3 + K'_\phi \cdot \phi + K'_{v|\phi} \cdot v'|\phi| + K'_{r|\phi} \cdot r'|\phi|) \quad (11)$$

$$= Y_H \times Z_H$$

where v', r' denote nondimensional lateral velocity, and yaw rate, respectively and are expressed as follows:

$$\dot{v}' = \frac{v}{U}, \quad \dot{r}' = \frac{rL_{pp}}{U} \quad (12)$$

Each maneuvering coefficient can be determined by circular motion test, or oblique towing test (OTT). For providing unified expressions, the nondimensional maneuvering coefficients are rewritten as follows:

$$X'_{vv} = \frac{X_{vv}}{\frac{1}{2}\rho L_{pp}d}, \quad X'_{vr} = \frac{X_{vr}}{\frac{1}{2}\rho L_{pp}^2d} \quad (13)$$

$$X'_{rr} = \frac{X_{rr}}{\frac{1}{2}\rho L_{pp}^3d}, \quad X'_{vvvv} = \frac{X_{vvvv}}{\frac{1}{2}\rho L_{pp}d/U^2} \quad (14)$$

$$Y'_v = \frac{Y_v}{\frac{1}{2}\rho L_{pp}dU}, \quad Y'_r = \frac{Y_r}{\frac{1}{2}\rho L_{pp}^2dU}, \quad Y'_\varphi = \frac{Y_\varphi}{\frac{1}{2}\rho L_{pp}dU^2} \quad (15)$$

$$Y'_{vv} = \frac{Y_{vv}}{\frac{1}{2}\rho L_{pp}d/U}, \quad Y'_{vr} = \frac{Y_{vr}}{\frac{1}{2}\rho L_{pp}^2d/U}, \quad Y'_{rr} = \frac{Y_{rr}}{\frac{1}{2}\rho L_{pp}^3d/U} \quad (16)$$

$$Y'_{rrr} = \frac{Y_{rrr}}{\frac{1}{2}\rho L_{pp}^4d/U}, \quad Y'_{v|\varphi|} = \frac{Y_{v|\varphi|}}{\frac{1}{2}\rho L_{pp}dU}, \quad Y'_{r|\varphi|} = \frac{Y_{r|\varphi|}}{\frac{1}{2}\rho L_{pp}^2dU} \quad (17)$$

$$N'_v = \frac{N_v}{\frac{1}{2}\rho L_{pp}^2dU}, \quad N'_r = \frac{N_r}{\frac{1}{2}\rho L_{pp}^3dU}, \quad N'_\varphi = \frac{N_\varphi}{\frac{1}{2}\rho L_{pp}^2dU^2} \quad (18)$$

$$N'_{vv} = \frac{N_{vv}}{\frac{1}{2}\rho L_{pp}^2d/U}, \quad N'_{vr} = \frac{N_{vr}}{\frac{1}{2}\rho L_{pp}^3d/U}, \quad N'_{rr} = \frac{N_{rr}}{\frac{1}{2}\rho L_{pp}^4d/U} \quad (19)$$

$$N'_{rrr} = \frac{N_{rrr}}{\frac{1}{2}\rho L_{pp}^5d/U}, \quad N'_{v|\varphi|} = \frac{N_{v|\varphi|}}{\frac{1}{2}\rho L_{pp}^2dU}, \quad N'_{r|\varphi|} = \frac{N_{r|\varphi|}}{\frac{1}{2}\rho L_{pp}^3dU} \quad (20)$$

$$K'_v = \frac{K_v}{\frac{1}{2}\rho L_{pp}d^2U}, \quad K'_r = \frac{K_r}{\frac{1}{2}\rho L_{pp}^2d^2U}, \quad K'_\varphi = \frac{K_\varphi}{\frac{1}{2}\rho L_{pp}d^2U^2} \quad (21)$$

$$K'_{vv} = \frac{K_{vv}}{\frac{1}{2}\rho L_{pp}d^2/U}, \quad K'_{vr} = \frac{K_{vr}}{\frac{1}{2}\rho L_{pp}^2d^2/U}, \quad K'_{rr} = \frac{K_{rr}}{\frac{1}{2}\rho L_{pp}^4d^2/U} \quad (22)$$

2.4 Propeller thrust and the hull resistance in still water

The surge force due to propeller thrust X_P with twin propellers is expressed as follows:

$$X_P = 2 \times (1 - t_p) T \quad (23)$$

$$T = \rho n_p^2 D_p^4 K_T(J_p) \quad (24)$$

$$J_p = \frac{(1 - w_p)u}{n_p D_p} \quad (25)$$

The hull resistance in still water R in the surge motion is expressed as follows:

$$R = \frac{1}{2} \rho S_F u^2 C_T \left(\frac{u}{\sqrt{gL_{pp}}} \right) \quad (26)$$

2.5 Hydrodynamic force by steering

The steering rudder forces components X_R, Y_R, N_R and K_R are expressed as follows:

$$X_R = -(1 - t_R) F_N \sin \delta \quad (27)$$

$$Y_R = -(1 + a_H) F_N \cos \delta \quad (28)$$

$$N_R = -(x_R + a_H x_{HR}) F_N \cos \delta \quad (29)$$

$$K_R = (z_R + a_H z_{HR}) F_N \cos \delta \quad (30)$$

where

$$F_N = \frac{1}{2} \rho A_R u_R^2 f_\alpha \sin \alpha_R \quad (31)$$

$$= \frac{1}{2} \rho (A_{RP} + A_{RS}) u_R^2 f_\alpha \sin \alpha_R$$

$$u_R = \varepsilon (1 - w_p) u \sqrt{\eta \left\{ 1 + \kappa \left(\sqrt{1 + \frac{8K_T(J_p)}{\pi J_p^2}} - 1 \right) \right\}^2 + 1 - \eta} \quad (32)$$

$$\alpha_R = \delta - \gamma_R \frac{U}{u_R} (\beta - \ell'_R r') \quad (33)$$

$$f_\alpha = \frac{6.13\Lambda}{2.25 + \Lambda}, \quad \varepsilon = \frac{1 - w_R}{1 - w_p} \quad (34)$$

$$\eta = \frac{D_p}{H_R}, \quad \beta = \arctan\left(\frac{-v}{u}\right), \quad U = \sqrt{u^2 + v^2} \quad (35)$$

2.5 Excited wave force

The wave-induced forces as the sum of the Froude-Krylov force (W_FK) and the diffraction force (W_Dif) including hydrodynamic lift forces acting on the hull are rewritten as follows. The rudder forces due to wave particle velocity which are considered for broaching prediction (Umeda & Hashimoto, 2002) are not taken into account for predicting pure loss of stability. The Froude-Krylov roll moment is taken into account for calculating the roll restoring force variation, so that only the diffraction force is used in Eq. (39).

$$X_W(\xi_G / \lambda, u, \chi) = X_{W_FK}(\xi_G / \lambda, u, \chi) \quad (36)$$

$$= -\rho g \zeta_w k \cos \chi \int_{AE}^{FE} C_1(x) S(x) e^{-kd(x)/2} \sin k(\xi_G + x \cos \chi) dx$$

$$Y_W(\xi_G / \lambda, u, \chi) = Y_{W_FK}(\xi_G / \lambda, u, \chi) + Y_{W_Dif}(\xi_G / \lambda, u, \chi)$$

$$= \rho g \zeta_w k \sin \chi \int_{AE}^{FE} C_1(x) S(x) e^{-kd(x)/2} \sin k(\xi_G + x \cos \chi) dx \quad (37)$$

$$+ \zeta_w \omega \omega_e \sin \chi \int_{AE}^{FE} \rho S_y(x) e^{-kd(x)/2} \sin k(\xi_G + x \cos \chi) dx$$

$$- \zeta_w \omega \sin \chi \left[\rho S_y(x) e^{-kd(x)/2} \cos k(\xi_G + x \cos \chi) \right]_{AE}^{FE}$$

$$\begin{aligned}
 N_w(\xi_G / \lambda, \chi) &= N_{w_FK}(\xi_G / \lambda, u, \chi) + N_{w_Diff}(\xi_G / \lambda, u, \chi) \\
 &= \rho g \zeta_w k \sin \chi \int_{AE}^{FE} C_1(x) S(x) e^{-kd(x)/2} x \sin k(\xi_G + x \cos \chi) dx \\
 &+ \zeta_w \omega \omega_e \sin \chi \int_{AE}^{FE} \rho S_y(x) e^{-kd(x)/2} x \sin k(\xi_G + x \cos \chi) dx \\
 &+ \zeta_w \omega u \sin \chi \int_{AE}^{FE} \rho S_y(x) e^{-kd(x)/2} \cos k(\xi_G + x \cos \chi) dx \\
 &- \zeta_w \omega u \sin \chi \left[\rho S_y(x) e^{-kd(x)/2} x \cos k(\xi_G + x \cos \chi) \right]_{AE}^{FE}
 \end{aligned} \quad (38)$$

$$\begin{aligned}
 K_w(\xi_G / \lambda, u, \chi) &= K_{w_FK}(\xi_G / \lambda, u, \chi) + K_{w_Diff}(\xi_G / \lambda, u, \chi) \\
 &= -\rho g \zeta_w k \sin \chi \int_{AE}^{FE} C_1(x) \frac{B(x)}{2} \{d(x)\}^2 e^{-kd(x)/2} \sin k(\xi_G + x \cos \chi) dx \\
 &- \rho g \zeta_w k^2 \sin \chi \int_{AE}^{FE} C_4(x) \left\{ \frac{B(x)}{2} \right\}^3 d(x) e^{-kd(x)/2} \sin k(\xi_G + x \cos \chi) dx \\
 &- \zeta_w \omega \omega_e \sin \chi \int_{AE}^{FE} \rho S_y I_\eta(x) e^{-kd(x)/2} \sin k(\xi_G + x \cos \chi) dx \\
 &+ \zeta_w \omega u \sin \chi \left[\rho S_y I_\eta(x) e^{-kd(x)/2} \cos k(\xi_G + x \cos \chi) \right]_{AE}^{FE} \\
 &+ Y_w(\xi_G / \lambda, u, \chi) \cdot \overline{OG}
 \end{aligned} \quad (39)$$

$$C_1 = \frac{\sin(k \sin \chi \cdot B(x) / 2)}{k \sin \chi \cdot B(x) / 2} \quad (40)$$

$$C_4 = \{k \sin \chi \cdot B(x) / 2\}^{-3} \left[2 \sin \{k \sin \chi \cdot B(x) / 2\} - k \sin \chi \cdot B(x) \cos \{k \sin \chi \cdot B(x) / 2\} \right] \quad (41)$$

2.6 Roll restoring force variation

Pure loss of stability is one of the problems related to the roll restoring force variation. The restoring force variation in oblique waves can be calculated by integrating the pressure around the instantaneously wetted hull surface with static balance of heave and pitch as show in Eq.(42) which is based on Froude-Krylov assumption (Lu et al., 2017). The Froude-Krylov roll moment is taken into account in Eq. (42) in oblique waves, while the effect of wave heading is converted into the change of the effective wave height in longitudinal waves by using Grim's effective wave concept in the references (Umeda & Yamakoshi, 1994; Kubo et al., 2012). For avoiding double counting of the Froude-Krylov roll moment in case of oblique waves, only the diffraction force is used in Eq. (39).

$$W \cdot GZ_w = \rho g \int_{AE}^{FE} y(x, \xi_G / \lambda) \cdot A(x, \xi_G / \lambda) dx + \rho g \sin \chi \cdot \int_{AE}^{FE} z(x, \xi_G / \lambda) \cdot F(x) \cdot A(x, \xi_G / \lambda) \cdot \sin(\xi_G + x \cos \chi) dx \quad (42)$$

$$F(x) = \zeta_w k \frac{\sin(k \frac{B(x)}{2} \sin \chi)}{k \frac{B(x)}{2} \sin \chi} e^{-k \cdot d(x)} \quad (43)$$

where, $A(x, \xi_G / \lambda)$ is the submerged area of local section of the ship. $y(x, \xi_G / \lambda)$ is the transverse position of buoyancy centre of local section.

$z(x, \xi_G / \lambda)$ is the vertical position of buoyancy centre of local section.

2.7 Roll damping force

Roll damping is one of essential terms for predicting roll motion, especially large amplitude roll motion. Linear and cubic nonlinear roll damping coefficients are used for predicting parametric roll and linear and squared nonlinear roll damping coefficients are used for predicting dead ship stability in the vulnerability criteria (IMO SDC 4, 2017). Linear and cubic nonlinear roll damping coefficients are adopted as shown in Eq.(44) for predicting pure loss of stability, which could lead to large amplitude roll motion, or even capsizing, in following and stern-quartering waves.

$$D(p) = (I_{xx} + J_{xx})(\alpha \cdot p + \gamma \cdot p^3) \quad (44)$$

3. SUBJECT SHIPS

The subject ship is the ONR Tumblehome vessel which is one of standard ships for the second generation intact stability criteria provided by the coordinator of corresponding group. The principal particulars and the lines of the ONR Tumblehome vessel are shown in Table 1 and Fig. 2, respectively.

Table 1 Principal particulars of the ONR tumblehome

Items	Ship	Model
Length:L	154.0m	3.800m
Draft:d	5.494m	0.136m
Breadth:B	18.8m	0.463m
Depth:D	14.5m	0.358m
Displ.:W	8507ton	127.8kg
C _B	0.535	0.535
GM	2.07m	0.044m
T _φ	12.38s	1.945s
κ _{yy}	0.25L	0.25L

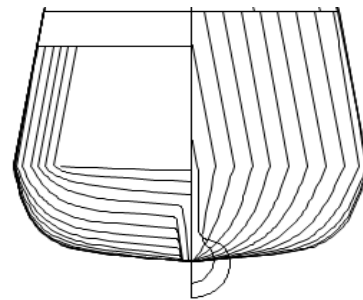


Fig.2 The ONR Tumblehome lines

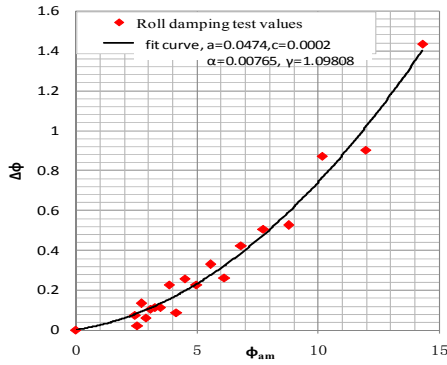


Fig.3 Extinction curve (a, c are linear and cubic extinction coefficients and α, γ are their nondimensional coefficients)

The nonlinear roll damping coefficients are obtained again from an existing model test (Gu et al., 2015) as shown in Fig.3.

4. SIMULATIONS AND DISCUSSIONS

The higher order maneuvering coefficients for hydrodynamic force acting on ship hull in the surge motion are taken into account in the MMG standard method for ship maneuvering prediction (Yasukawa & Yoshimura, 2015), and the higher order maneuvering coefficients without X_{vvv} are also recommended for predicting pure loss of stability by Japan (IMO SLF55, 2013; Kubo et al., 2012), while these higher order maneuvering coefficients are ignored for broaching prediction (Umeda et al., 2016). For investigating the effect of higher order maneuvering coefficients in the surge motion on predicting pure loss of stability, the following value $X'_{vv} = -0.040$, $X'_{vr} = -0.0622$, $X'_{rr} = 0.00841$, $X'_{vvv} = 0.771$ are used based on databases of ships.

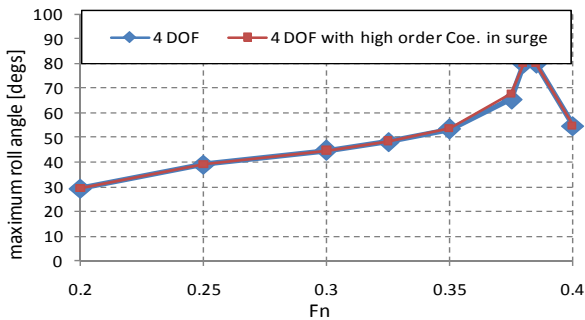


Figure 4 Comparison of maximum roll angle as function of the Froude number between the 4 DOF without and with higher order coefficients in the surge motion with $\lambda/Lpp=1.25$, $H/Lpp=0.05$, and $\chi=30^\circ$.

A comparison of maximum roll angle as function of the Froude number between the 4 DOF with and without higher order coefficients in the surge motion under the condition of $\lambda/Lpp=1.25$, $H/Lpp=0.05$, and $\chi=30^\circ$.

$Lpp=0.05$, and $\chi=30^\circ$ are carried out as shown in Fig.4. The results indicate that the effect of higher order maneuvering coefficients in the surge motion on predicting pure loss of stability is very small. The higher order maneuvering coefficients in the surge motion are ignored in following simulations.

The higher order maneuvering coefficients of heel-induced hydrodynamic forces are not considered in this study due to lack of referenced databases of ships. The other maneuvering coefficients mentioned in the references (Hashimoto et al., 2011b; Umeda et al., 2016) are used in this study.

For investigating the effect of different mathematical models on predicting pure loss of stability, a comparison of maximum roll angle as function of the Froude number between mathematical models with different DOF are conducted as shown in Fig.5.

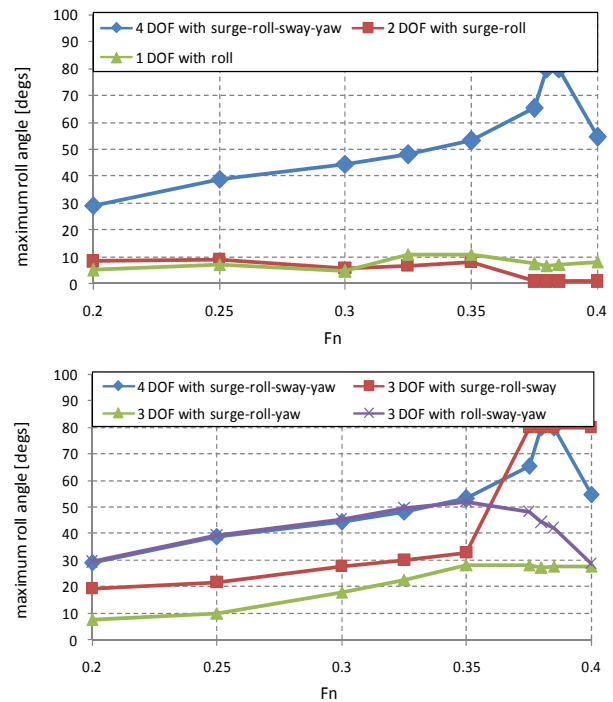


Figure 5 Comparison of maximum roll angle as function of the Froude number between mathematical models with different DOF with $\lambda/Lpp=1.25$, $H/Lpp=0.05$, and $\chi=30^\circ$.

The mathematical models with 1 DOF of roll motion and 2 DOF of surge-roll coupled motion could underestimate the roll angle and fail to predict capsizing due to pure loss of stability in stern-quartering waves. The mathematical model with 3 DOF of roll-sway-yaw coupled motion could predict the roll angle, but it also fails to predict capsizing at critical ship speeds due to pure loss of

stability. This means the surge motion is very important for predicting capsizing at critical ship speeds due to pure loss of stability. The surge motion cannot be ignored in the mathematical model for predicting pure loss of stability, that is to say, the forward speed effect on pure loss of stability in stern-quartering waves should be considered.

The roll angle predicted by the mathematical model with 3 DOF of surge-roll-yaw coupled motion is generally larger than that with 2 DOF of surge-roll coupled motion, but it also fails to predict capsizing at critical ship speeds due to pure loss of stability. The mathematical model with 3 DOF of surge-roll-sway coupled motion could also underestimate the roll angle, but it overestimates the capsizing range of critical ship speeds due to pure loss of stability. The mathematical model with 4 DOF of surge-roll-sway-yaw coupled motion could predict roll angle and appropriately estimate capsizing range of critical ship speeds due to pure loss of stability. This also supports the conclusion in the reference (Kubo et al., 2012) that the centrifugal force due to sway and yaw motions, other than the restoring reduction on a wave crest, are indispensable for explaining “pure” loss of stability on a wave crest. Therefore, both the sway and yaw motions should be considered in the mathematical model for predicting pure loss of stability.

The higher order maneuvering coefficients for hydrodynamic force acting on ship hull could affect predicting pure loss of stability, and a comparison of maximum roll angle between the 4 DOF with and without high order coefficients in roll, sway and yaw motions under the condition of $\lambda/Lpp=1.25$, $H/Lpp=0.05$, and $\chi=30^\circ$ are carried out as shown in Fig.6.

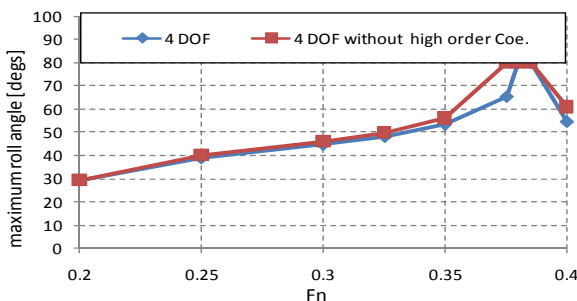


Figure 6 Comparison of maximum roll angle as function of the Froude number between the 4 DOF with and without higher order maneuvering coefficients in roll, sway and yaw motions with $\lambda/Lpp=1.25$, $H/Lpp=0.05$, and $\chi=30^\circ$.

The results indicate that the mathematical model of 4 DOF without higher order maneuvering

coefficients in sway, yaw and roll motions could predict roll angle, but it could overestimate the capsizing range of critical ship speeds due to pure loss of stability.

Diffraction forces are very important for predicting ship motions in waves, and for investigating the effect of diffraction forces on predicting pure loss of stability in stern-quartering waves, simulations with diffraction forces, without diffraction forces and only without diffraction forces in the roll motion are carried out as shown in Fig.7. The mathematical model of 4 DOF without diffraction forces could underestimate roll angle due to indirectly reducing the effect of maneuvering motions on the roll and it also fails to correctly predict capsizing range of critical ship speeds. The mathematical model of 4 DOF only without diffraction forces in the roll motion could estimate roll angle, but it completely fails to predict capsizing at critical ship speeds. This means diffraction forces should be taken into account for predicting pure loss of stability in stern-quartering waves.

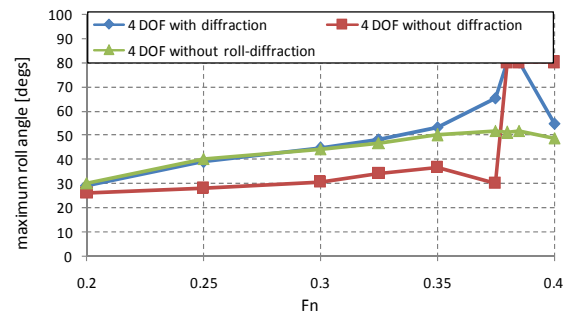


Figure 7 Comparison of maximum roll angle as function of the Froude number between with forces, without diffraction forces and only without diffraction forces in the roll motion with $\lambda/Lpp=1.25$, $H/Lpp=0.05$, and $\chi=30^\circ$.

Pure loss of stability is accompanied with large roll. The heel-induced hydrodynamic forces for large heel angle in calm water, which are hydrodynamic lift due to underwater non-symmetry induced by heel angle with forward velocity, could affect the prediction of pure loss of stability. The linear heel-induced hydrodynamic forces in calm water are investigated as shown in Fig.8. The 4 DOF mathematical model without linear heel-induced hydrodynamic forces, such as $Y'_\varphi \cdot \varphi$, $N'_\varphi \cdot \varphi$, $K'_\varphi \cdot \varphi$, could fail to predict capsizing at critical ship speeds due to pure loss of stability.

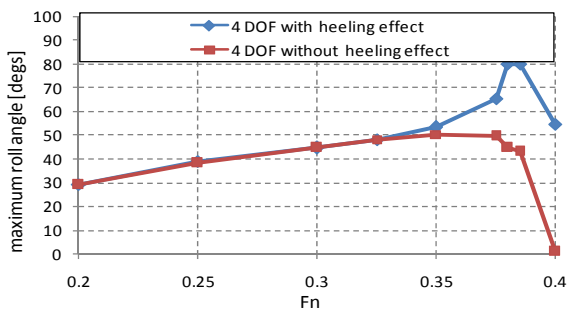


Figure 8: Comparison of maximum roll angle as function of the Froude number between the 4 DOF with and without linear heeling effect with $\lambda/Lpp=1.25$, $H/Lpp=0.05$, and $\chi=30^\circ$.

Roll damping is one of essential terms for predicting large amplitude roll motion, such as parametric roll, roll under dead ship condition and roll due to pure loss of stability. Linear and cubic nonlinear roll damping coefficients are adopted for predicting parametric roll (IMO SDC 4, 2017). The effects of nonlinear damping coefficient with linear and cubic nonlinear roll damping and equivalent linear roll damping coefficient on predicting pure loss of stability are investigated as shown Fig.9. Here the equivalent linear roll damping coefficient are derived by $a_e = a + c \cdot \phi_a = a + c \cdot 20$. It shows that the 4 DOF mathematical model with equivalent linear roll damping coefficient could overestimate the capsizing range of critical ship speeds.

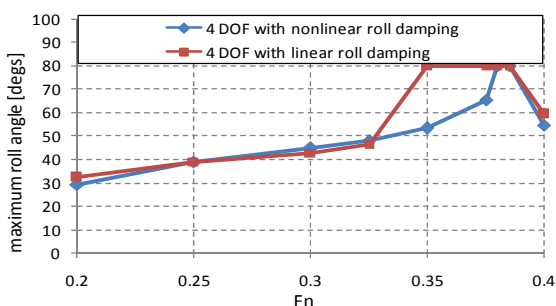


Figure 9: Comparison of maximum roll angle as function of the Froude number between the 4 DOF with nonlinear damping and linear damping with $\lambda/Lpp=1.25$, $H/Lpp=0.05$, and $\chi=30^\circ$.

5. CONCLUSIONS

On the basis of the numerical study on standard mathematical model of pure loss of stability in stern-quartering waves with the ONR tumblehome vessel, the following remarks can be made:

1) The effect of surge motion with varied forward speed effect on pure loss of stability in stern-quartering waves should be considered while the

higher order maneuvering coefficients in the surge motion can be ignored.

2) The centrifugal force due to sway and yaw motions and maneuvering motions with higher order maneuvering coefficients should be considered in the standard mathematical model of pure loss of stability.

3) The effect of linear heel-induced hydrodynamic forces in calm water on pure loss of stability in stern-quartering waves should be taken into account.

4) The nonlinear roll damping coefficient should be included for predicting pure loss of stability in stern-quartering waves.

The standard mathematical model with 4 DOF for predicting pure loss of stability should be further studied with experiments and more examples.

Acknowledgments

Some contents used in this research were once guided by Prof. Naoya Umeda during the first author's Ph.D course at Osaka University supported by China Scholarship Council [No.2008606031]. The research is supported by Ministry of Industry and Information Technology of China (No. [2016] 26) and China research fund (No.B2420132001; No.51509124). These supports are gratefully acknowledged.

6. REFERENCES

Gu M., Lu J. and Wang T.H., 2015, "Stability of a Tumblehome Hull under Dead Ship Condition", *Journal of Hydrodynamics*, Vol.27 (3), pp. 452-457.

Hamamoto M., Kim Y.S., 1993, "A New Coordinate System and the Equations Describing Maneuvering Motion of a Ship in Waves", *Journal of the Society of Naval Architects of Japan*, Vol. 173, pp. 209-220.

Hashimoto H., Umeda N. and Matsuda A., 2004, "Importance of Several Nonlinear Factors on Broaching Prediction", *Journal of Marine Science and Technology*, Vol. 9, pp. 80-93.

Hashimoto H., Umeda N. and Matsuda A., 2011a, "Model Experiment on Heel-Induced Hydrodynamics Force in Waves for Realising Quantitative Prediction of Broaching", *M.A.S. Neves et al. (eds.), Contemporary Ideas on Ship*

Stability and Capsizing in Waves, Fluid Mechanics and Its Application 96, pp. 379-397.

Hashimoto H., Umeda N. and Matsuda A., 2011b, "Broaching Prediction of a Wave-piercing Tumblehome Vessel with Twin screws and Twin Rudders", Journal of Marine Science and Technology, Vol. 16, pp. 448-461.

IMO2013, Development of Second Generation Intact Stability Criteria, SLF55/INF.15. Annex 12

IMO2016, Finalization Second Generation Intact Stability Criteria, SDC 3/WP.5. Annex 3

IMO 2017, Finalization Second Generation Intact Stability Criteria, SDC 4/WP.4.

Kubo H., Umeda N., Yamane K., Matsuda A., 2012, "Pure Loss of Stability in Astern Seas -Is It Really Pure?", Proceedings of the 6th Asia-Pacific Workshop on Marine Hydrodynamics, pp. 307-312.

Lu J., Gu M. and Umeda N., 2017, "Experimental and Numerical Study on Several Crucial Elements for Predicting Parametric Roll in Regular Head Seas", Jour. of Marine Science and Technology, Vol. 22, pp. 25-37.

Matsuda A. and Umeda N., 1997, "Vertical Motions of a Ship Running in Following and Quartering Seas", Naval Architecture and Ocean Engineering, No.227, pp.47-55(in Japanese).

Umeda N., 1999, "Nonlinear Dynamics of Ship Capsizing due to Broaching in Following and Quartering Seas", Journal of Marine Science and Technology, Vol. 4, pp. 16-26.

Umeda N. and Hashimoto H., 2002, "Qualitative Aspects of Nonlinear Ship Motions in Following and Quartering Seas with High Forward Velocity", Journal of Marine Science and Technology, Vol. 6, pp. 111-121.

Umeda N., Usada S., Mizumoto K., and Matsuda A., 2016, "Broaching Probability for a Ship in Irregular Stern-quartering Waves: Theoretical Prediction and Experimental Validation", Journal of Marine Science and Technology, Vol. 21, pp. 23-37.

Yasukawa H. and Yoshimura Y., 2015, "Introduction of MMG Standard Method for Ship Maneuvering Predictions", Journal of Marine Science and Technology, Vol. 20, pp. 37-52.

Umeda N. and Yamakoshi Y., 1994, "Probability of Ship Capsizing due to Pure Loss of

Stability in Quartering Seas", Naval Architecture and Ocean Engineering, Vol.30, pp.73-85.